

## Estimating Disease Severity of Single Plants

S. E. Lindow

Associate professor, Department of Plant Pathology, University of California, Berkeley 94720.

The individual research reported in this review was supported in part by a grant from the California Department of Food and Agriculture. Technical assistance and suggestions by R. R. Webb and G. Anderson are gratefully acknowledged. I also wish to thank S. Scalise for valuable assistance in the assembly language programming used in this report, K. Callan for assistance with photography, and J. Loper for critical review of the manuscript.

Accepted for publication 24 May 1983.

Accurate measurements of disease severity are important in any study relating disease severity to disease losses. Accurate measurements of disease severity are also very important in developing epidemiological models useful for predicting disease losses in food crops. Sherwood et al (28) have shown that errors in measurement of disease severity cause estimates of temporal disease progress to differ significantly from the true rate of disease increase.

Many of the procedures used for estimating disease severity are either subjective or qualitative and thus do not satisfy the exacting requirements for quantitative estimates of disease severity. Although accurate measurements of disease severity are required in studies determining disease losses, few workers (12,13,28) have given critical attention to the accuracy or precision of these estimates.

**Visual assessment of disease severity.** Until recently, visual estimates of disease severity have been used almost exclusively. Many different methods of estimating disease severity developed by various workers are described in recent reviews (2,6,17,18). Although these methods often are useful in collecting data for studies of disease-loss appraisal, epidemiology, or disease resistance, they are not sufficient for all purposes. The specificity of these methods to a given disease or the difficulty of their application have limited their adoption by other workers (6,17).

Methods for visual assessment of disease generally fall into two categories. In the first category are pictorial descriptive keys that show plants with varying amounts or types of disease symptoms (17). This type of visual key for assessing disease severity are exemplified by those used for assessing late blight of potato which is caused by *Phytophthora infestans* (Mont) de Bary (1) or blight diseases of corn (30). Such visual assessment keys have been used successfully by single observers to estimate disease intensity of host plants of differing disease resistance, or of host plants subjected to differing environmental conditions or cultural procedures. Since visual assessment keys often set arbitrary levels of disease severity based upon symptomatology, several problems exist. Different observers using the key to evaluate diseased plants of similar symptomatology do not always obtain similar estimates of disease severity. In a detailed study, Sherwood et al (28) demonstrated that experienced observers utilizing identical assessment keys generated significantly different disease estimates for a set of diseased leaves. A key designed to estimate disease severity based upon symptomatology of one plant cultivar may not be applicable to the disease symptoms manifested on other plant cultivars. Finally, the use of these keys does not allow easy interpolation of intermediate levels of disease severity.

Visual methods of disease assessment in the second category utilize standard area diagrams. Pictorial representations of the host plant with known and graded amounts of disease are compared with diseased leaves to allow estimation of disease severity. Excellent reviews on the use and construction of standard area diagrams have been written by James (16,17). Examples of

standard area diagrams in current use include those for apple scab (8,18), common scab of potato (16,20), and wheat rust (7,24,27). The Cobb scale for assessment of wheat rust was among the first of the standard area diagrams that have been developed and is superior to later versions of this scale because estimated disease severity is proportional to the absolute area of the leaf that is diseased, and not expressed as a percentage of an arbitrary maximum severity value (17). In contrast to visual assessment keys, standard area diagrams allow estimation of intermediate levels of disease severity by comparing a diseased plant with diagrams showing both more and less disease.

In 1945, Horsfall and Barratt (13), noting the Weber-Feckner law, emphasized the limitations of the eye as a sensing device in the assessment of plant disease. The Weber-Feckner law states that the visual acuity of the eye is proportional to the logarithm of the intensity of the stimulus. These authors also noted that in visually estimating disease severity, the observer actually assesses the diseased portion of leaves having <50% injury and the healthy portion of leaves having >50% injury (12,13). Horsfall and Barratt developed a disease-rating scale containing 12 equal divisions of disease severity on a logarithmic scale with a median value of 50%. Thus, divisions of this scale included decreasing ranges of disease severity when either increasing or decreasing from 50% disease severity (12). This scale (12,13) and many standard area diagrams constructed recently (17,19) account for the logarithmic decrease in acuity of the eye in estimating disease severities approaching 50% in their selection of representative keys. Estimations of disease severity intermediate between two keys are made by careful interpolation (17). However, the errors in such estimates are maximum at disease severities approaching 50%.

Visual estimates of disease severity can differ significantly from the true amount of disease. If the observer was not subject to limitations in visual acuity at the midrange of disease severity, estimated disease severity and actual disease severity would be linearly related, and the variance of estimates would be independent of disease severity (Fig. 1). However, the Weber-Feckner law indicates that the true confidence interval of estimates of disease severity approach the expected linear relationship at both low and high disease levels, but depart increasingly from this line with increasing disease severity with a maximum variance at 50% disease (Fig. 1). Serious errors in predictions of yield losses or other functions of disease severity result because errors in visual estimates of disease severity are not independent of the level of disease.

The pattern of disease symptoms on plant parts can also influence visual estimates of disease severity. In a detailed study, Sherwood et al (28) demonstrated that the number of lesions on a plant part biased disease severity estimates generated by most observers. Regression analysis showed that errors in disease estimates were directly related to the number of lesions on a leaf (28). The irregular bipinnately compound leaves of the bracken fern (*Pteridium aquilinum* L. Kuhn) as well as the irregular lesions caused by *Ascochyta pteridis* Bres. on this host (32) (Fig. 2) make this disease especially difficult to evaluate by using pictorial assessment keys (22). These factors caused differing amounts of bias in estimates of severity of lesions on bracken fern depending upon the level of disease severity (S. E. Lindow, unpublished).

The publication costs of this article were defrayed in part by page charge payment. This article must therefore be hereby marked "advertisement" in accordance with 18 U.S.C. § 1734 solely to indicate this fact.

Errors in visual estimates of disease severity increased with increasing disease severity to about 50% frond area infected, as expected from the limitations in visual estimates described in Fig. 1.

**Remote sensing and analysis of photographs of diseased plants.**

Remote sensing procedures have proven valuable in assessment of plant disease. False-color aerial infrared photography has been the remote sensing procedure most commonly utilized to detect plant diseases (4,5,11,14,15,26,29,31). The detection of diseased plant tissue on false-color infrared film is due to its greater reflection of near infrared light ( $\lambda = 700-950$  nm) compared to healthy tissue (10). Color infrared photographs have been analyzed with microdensitometers or other types of electronic scanning devices to quantitate disease severity (29,31). Because most aerial infrared photographs are taken from altitudes ranging from 100 to 20,000 m, the resolution of such photographs is usually low, allowing estimates only of disease incidence and not severity (29). However, severity estimates of diseases not occurring in foci have been made for whole fields from analysis of color infrared photographs (26). The high cost and inconvenience of taking and analyzing color infrared photographs has limited the employment of this method for estimating disease severity of single plants or leaves.

Disease severity of single plants has been assessed accurately by analysis of photographs of the plants (9). Photographic 35-mm transparencies of cleared wheat leaves infected by *Septoria tritici* were scanned with a television beam to quantitate the area of infected tissues and the area of individual pycnidia. The inconvenience of clearing and photographing individual leaves and the need for specialized electronic equipment has restricted the use of this procedure for assessment of disease severity of single plants. Although the analysis of photographs of diseased plants is very accurate, a more convenient and versatile automated disease assessment procedure would be desirable.

**Microcomputer-controlled digital video image analysis.**

Recently, video image analysis has been used for assessment of plant disease severity (3,21,22,25). Video image analysis avoids some of the problems inherent in visual analysis of plant disease severity because the response to an optical stimulus is more nearly linear with intensity. Recent advances in electronic and computer technology allow video cameras to interface directly with a microcomputer. Rapid, automated, nonsubjective estimates of disease severity are made possible by computer-controlled analysis of video images. The analysis of video images is useful for the assessment of only those plant diseases with lesions having a different color from healthy tissue, or those with lesions that can be contrasted with healthy tissue by optical procedures (3,22,25). Commercially available video image systems have accurately estimated the extent of wood decay of stained cross sections of trees (3) and the severity of foliar diseases from samples of individual

leaves or from photographs of leaves or groups of plants (25). Although these systems provide the technology needed for a major advancement in disease assessment, they are either relatively insensitive (resolution of only eight shades of grey) and inflexible (3), or quite expensive ([25]; and H. Nilsson, *personal communication*).

**Apple II-controlled digital video image analysis.** An automated disease assessment device has been developed that interfaces an inexpensive Apple II Plus microcomputer (Apple Computer, Inc., Cupertino, CA 95014) with a closed circuit television camera, or video tape recorder via a DS-65 analogue-to-digital converter (The MicroWorks, Del Mar, CA 92014) (22). Most video images are a composite of a series of 254 lines and 254 columns which comprise a collection of some 64,000 individual picture elements (pixels). To assess leaf area and necrotic tissue area, video images are digitized and the data processed by a microcomputer. Individual picture elements in the video image are located, and pixel intensity quantified by using the DS-65 digisector video digitizer interfaced with an Apple II Plus microcomputer. The DS-65 video digitizer converts an analog signal of a given pixel to a digital value with a resolution of 64 levels of grey (from 0 for black to 63 for white). The variable contrast adjustment on the DS-65 peripheral is set at minimum contrast for optimum performance. Individual pixels at predetermined locations in the video image are located and digitized under BASIC and Assembly language program control by the Apple II computer. Thus, either all or a predetermined subset of the pixels comprising a video image are selected for further analysis. Assembly language programs were written to allow rapid addressing and retrieval of digitized pixels for routine operation of the disease assessment device. Both Assembly and BASIC

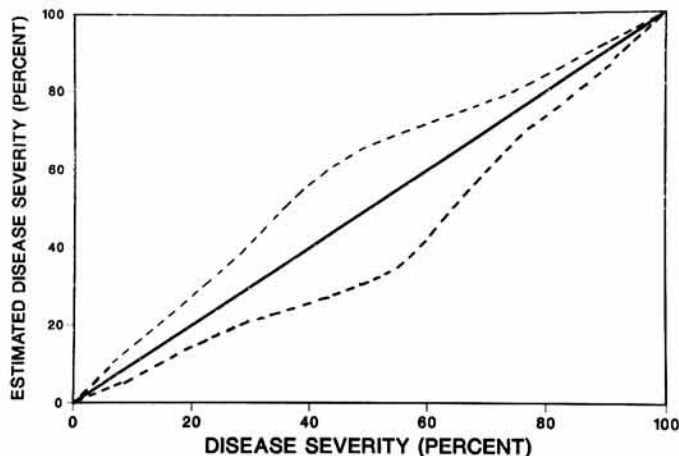


Fig. 1. Relationship between true disease severity (abscissa) and visually estimated severity of disease (ordinate) with no error in estimates (—) and confidence limit of estimates with error a function of the logarithm of disease severity (----).



Fig. 2. Irregular shape and distribution of dark necrotic lesions on bracken fern infected by *Ascochyta pteridis*.



programming codes and data are readily stored, changed, and retrieved for execution from a floppy disk subsystem of the Apple II computer.

Correct operation of the automated disease assessment device requires contrast in brightness between the video image of healthy and diseased plant tissue and between plant tissue and background material. Sufficient contrast between these objects on leaves having relatively light-colored lesions is obtained by illumination of plant material placed on a black velvet surface in a light-tight box with red light ( $\lambda > 620 \mu\text{m}$ ) to minimize visible fluorescence and to enhance brightness contrast between green and nongreen (red light reflecting) plant tissue. A red filter placed over the lens of the portable camera operated in sunlight may also maximize contrast between healthy and diseased tissue photographed in the field. A continuous video image of plant tissues is generated with a black-and-white video camera (RCA model TC 2011) equipped with an 8-mm wide-angle video lens (22) or with a portable color video camera (Panasonic model PK-801). Optimum camera performance is achieved by operation of the camera with the automatic gain control off, with the peak averaging controls responsive only to average scene brightness, and with the gamma controls set to reduce contrast in the darker areas of the picture. Sufficient contrast between healthy plant tissue and diseased tissue having darkly pigmented lesions is achieved by placing diseased leaves on a light grey background material, and by placing a yellow filter over the lens of the video camera.

Sorting of pixels of a video image according to magnitude (shade of grey) permits the estimation of leaf area and area of necrotic lesions. Pixel intensities corresponding to video images of background, healthy, and diseased plant tissue are placed in one of three defining categories (22). Two pixel thresholds (three categories of pixel intensity in the range from 0 to 63) are adjusted to minimize the number of improperly grouped pixels. The determination of the two pixel intensity thresholds is simplified by depicting pixels of each of three different intensity ranges in one of three colors on the Apple II video monitor. Both pixel intensity thresholds are then adjusted until an image corresponding to diseased and healthy tissue on a uniform background is clearly depicted on the Apple II video monitor. Most pixels from images of healthy green leaf tissue commonly have magnitudes  $>5$ , but  $<45$ , while most pixels from images of necrotic leaf tissues have magnitudes either  $>45$  (light-colored lesions) or  $<5$  (darkly pigmented lesions). A regular array containing 16,232 individual pixels of an entire video image can be located, digitized and grouped into each of the above three categories in 3.7 sec. The fraction of total pixels grouped into the three magnitude categories corresponding to background, healthy and necrotic leaf tissues yield an initial approximation of the proportion of the video image corresponding to each of these three objects. Factors contributing to variance in the area determinations include light intensity, camera aperture and performance, and the type of plant, ie, the shade of green of healthy leaf being examined.

Corrections to the initial area approximations are made by separately estimating the fraction of pixels incorrectly assigned to a given category. Prior to analysis of a given plant species, a small area of the video image delimited by 992 pixels occupied exclusively by healthy leaf tissue of this species is digitized and categorized into the three magnitude categories. This analysis yields an estimate of the small fraction of pixels corresponding to healthy leaf tissue that would otherwise be incorrectly grouped in the category corresponding to the background. Similarly, another initial analysis of approximately 9,000 pixels occupied by healthy leaf tissue of a given plant species yields an estimate of the small fraction of pixels that would be incorrectly grouped into the category corresponding to necrotic leaf tissue. An area containing 992 pixels in the corner of the video image occupied exclusively by uniform background also is automatically digitized prior to and following each analysis of an entire video image containing both healthy and necrotic leaf tissue on a uniform background. An analysis of this background at each determination allows estimation of the small fraction of pixels corresponding to background that would be incorrectly grouped in a category corresponding to healthy leaf

tissue.

Determination of the areas of healthy leaf and necrotic leaf tissues can be summarized in the following five steps. First, initial estimates of the background, healthy leaf, and necrotic leaf areas are obtained by digitizing a specific portion of the video image and grouping the individual pixels into three magnitude categories. Second, correctional algorithms under BASIC programming control, utilizing initially determined estimates of the portion of healthy leaf incorrectly categorized as either background or diseased leaf tissue, as well as estimates of background incorrectly categorized as healthy leaf tissue, are employed to yield final corrected estimates of the total video image corresponding to background, healthy, or necrotic leaf tissue. Third, computational algorithms, including those describing the area observed by the video camera as a function of distance, are utilized to calculate areas of leaves and/or necrotic lesions. Availability of a value for average lesion size also permits calculation of the number of lesions per leaf. Fourth, final results of a given sample are displayed on a second video monitor, printed on a hard copy printer, and stored in the memory and in a floppy disk subsystem of the Apple II computer. Finally, statistical calculations utilizing stored data are automatically computed in real time under BASIC programming control following completion of each experiment. A single determination of leaf area and necrotic leaf area including estimation of error factors and correctional and computational algorithms requires 4.1 sec (22). A set of 100 individual leaves or plants placed before a laboratory based video camera or remotely recorded video images (Fig. 3) can be processed in less than 45 min.

Fluctuations in light intensity and camera performance as well as differences in green pigmentation in healthy leaves due to varietal or cultural differences require that automatic corrections be made to ensure reproducibility of determinations. Correctional factors obtained from the initial distribution of pixel magnitudes of healthy leaves and automatic analysis of pixel magnitudes of the dark background in each determination greatly reduce variability in system performance. The average extreme determination of total or necrotic leaf area differed from the mean of five successive observations of a given leaf by only 0.8% (22).

Increases in system performance with increasing numbers of pixels analyzed is associated with progressively longer execution times. Analysis of approximately 25% of the total pixels in each video image was chosen as an acceptable compromise on system performance and efficiency. Only small improvements in the resolution and reproducibility of the automated disease assessment system were obtained by increasing the number of pixels digitized and categorized from the 16,232 routinely analyzed.

The automated disease assessment device performed well on intact potted plants as well as on detached leaves. Average disease severity was determined by reading several leaves simultaneously with error approaching those of single leaves if the potted plant was illuminated with a uniform and diffuse light source.

The total area of healthy and lightly colored diseased tissue of several plant species calculated from analysis of laboratory-based camera-generated video images very closely matched the actual areas as determined with a planimeter (22). The accuracy of assessment of total and diseased leaf areas was independent of leaf size or disease severity (22). The average error in calculation of pinto bean (*Phaseolus vulgaris*) leaf area from digital image analysis was approximately 1.2%. Total leaf areas of other plants with highly irregular leaves such as bracken fern or tomato (*Lycopersicon esculentum* L.) were also computed from video image analysis with an accuracy of greater than 98.0%. The diseased areas of leaves of tomato infected with *Alternaria solani* Ell. & G. Martin, bracken fern infected with *A. pteridis*, sycamore (*Platanus racemosa* Nutt.) infected with *Microspora alni* DC ex Wint., and California buckeye (*Aesculus californica* (Spach) Nutt.) with marginal leaf necrosis were highly correlated (coefficient of determination = 0.97;  $P < 0.01$ ) with the actual areas of diseased tissue. Estimates of necrotic frond area based on visual assessment keys were much less precise than estimates made from video image analysis (22). Whereas estimates of diseased leaf area from visual assessment keys approached those obtained from video image

analysis and those determined with a planimeter at both low and very high disease severity, large errors were incurred at intermediate disease severity levels (22).

The accuracy of estimates of disease severity obtained using video image analysis was high and appeared independent of both the complexity of the host-pathogen system and disease severity. Regressions of disease severity estimated by the automated disease assessment device to disease severity determined with a planimeter had slopes very close to 1.0. The 95% confidence limits for



**Fig. 3.** Analysis of remotely recorded video images for estimating disease severity. **A.** Operation of hand-held portable color video camera focused on a group of four to six leaves with a black velvet tarp as a background. Images are shown recorded on a portable video cassette recorder. **B.** Analysis of recorded images stored on video tape (1) linked to the Apple II Plus computer (2) and a video monitor (3). Analyzed data or false-color representation of pixel intensity are displayed on another video monitor (4) or results of individual measurements are printed (5).

individual determinations averaged within  $\pm 2.0$  percent of the expected value obtained by regression for each of the four diseases examined with laboratory-based cameras.

The area of darkly pigmented lesions on leaves was also accurately measured by analysis of video images. The percentage leaf area of *Raphiolepis indica* (L.) Lindl. leaves with dark brown spots caused by *Entomosporium maculatum* Lev. calculated with the automated disease assessment device was highly correlated with the actual percentage diseased area (Fig. 4). Similarly, the area of dark red marginal necrosis caused by water stress on leaves of liquidambar (*Liquidambar styraciflua* L.) were also highly correlated with the actual necrotic leaf areas (Fig. 4). As with relatively lightly pigmented lesions, the 95% confidence limits for individual determinations of dark lesion areas averaged within 1.8% of the expected value. Error in estimating severity of darkly colored diseased tissue was independent of true disease severity (Figs. 4 and 5).

While the speed and accuracy of the laboratory-based automated disease assessment device should make it useful for evaluation of the hundreds of leaves that may be required for a systematic

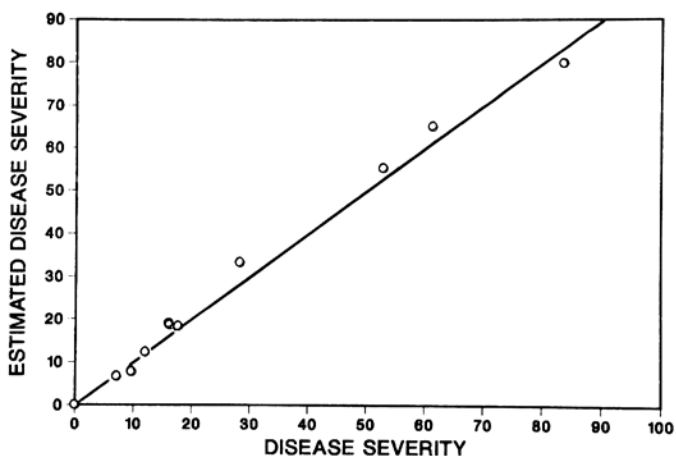


**Fig. 4.** Relationship between percent of *Liquidambar styraciflua* leaves covered with dark marginal necrosis as determined from dissection and weighing of enlarged black-and-white photographs of leaves (abscissa) and as computed by video image analysis (ordinate) of recorded images of leaves. The line drawn represents the linear regression  $Y = 0.99X - 0.91$ ; coefficient of determination = 0.996 ( $P < 0.01$ ).

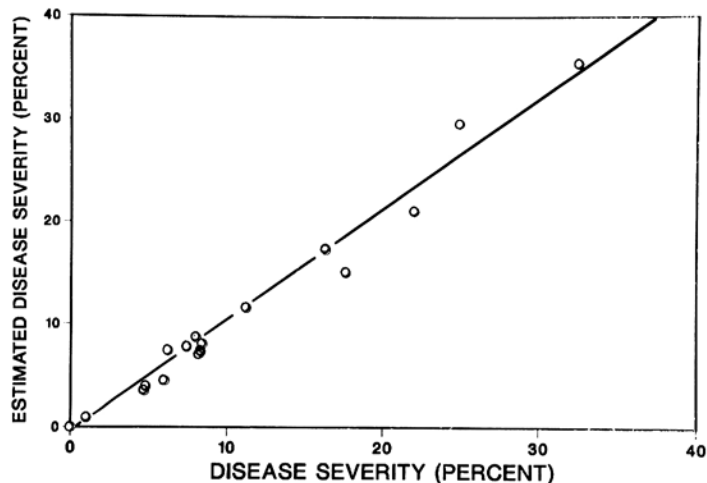


**Fig. 5.** Relationship between percent of leaf area of *Raphiolepis indica* with dark necrotic spots as determined by dissection and weighing of enlarged black-and-white photographs of diseased leaves (abscissa) and as computed by video image analysis (ordinate) of recorded images (JVC model HR-2200U portable color video cassette recorder). The line drawn represents the linear regression  $Y = 1.10X - 1.03$ ; coefficient of determination = 0.988 ( $P < 0.01$ ).

sampling of field material (2), there are limitations to this procedure. For example, many types of field-grown plants are too fragile to transport to the laboratory for analysis by a laboratory-based video camera. This problem can be overcome by recording images of diseased plants remotely and analyzing the recorded video image in the laboratory. The percentage leaf area of *Quercus lobata* Nee covered with mycelia of *Sphaerotheca lonestris* Harkn. was calculated from analysis of remotely recorded video images of diseased leaves and was correlated with the actual area of fungal colonization (Fig. 6).

Analysis of remotely recorded video images to assess disease severity has several advantages to laboratory-based video cameras: average estimates of disease severity can be made readily by observation of several leaves or plants simultaneously; perishable or sporulating plant material can be observed in situ; repeated observation of the same plant tissues can be made due to the nondestructive nature of the remotely recorded video images.

The microcomputer-directed video image analysis system discussed here was shown to be more accurate and reproducible in quantifying severity of foliar diseases than the visual assessment keys used currently (22). The microcomputer-controlled automated disease assessment device was designed to be largely self-correcting for variations in system performance and among the diseases under investigation. Internal correction algorithms utilized by the computer maximize reproducibility with a 95% confidence interval of <1.0%.

Additional improvements in system performance could be accomplished by initiating optical changes such as measuring near-infrared radiation instead of different visible wavelengths. Manzer and Cooper (23) have recently reported success in observing potato late blight symptoms by remote observation of potato fields with a video camera responsive to near-infrared light. Interfacing such a modified video camera to the microcomputer-controlled video image analysis system described here may increase the sensitivity and versatility of this procedure.

The accuracy of estimates of foliar disease severity obtained by video image analysis varies inversely with the dimensions of the plant sample being analyzed. Increasing the number of leaves or plants included in one observation will reduce the accuracy of mean disease severity estimations. Therefore, a more accurate determination of mean disease severity may be obtained by randomly sampling a larger number of individual leaves or plants. The speed and accuracy of the automated disease assessment device would be ideal for such a purpose. The video image analysis system described is useful for determining disease severity on a large number of individual leaves to determine average disease severity

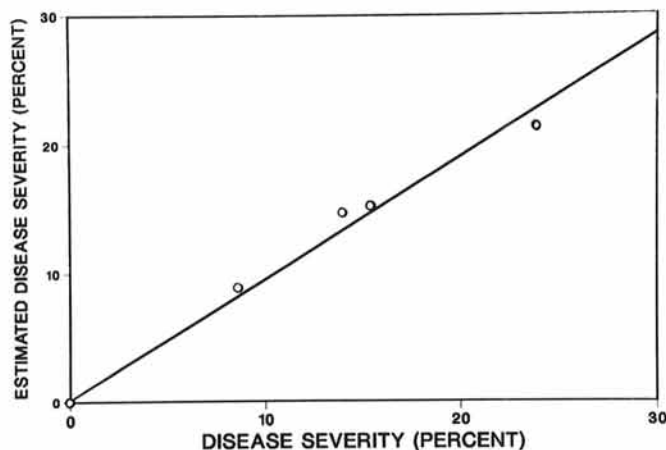


Fig. 6. Relationship between percent of oak (*Quercus lobata*) leaf area covered with mycelia and conidia of *Sphaerotheca lonestris* as determined from dissection and weighing of enlarged black-and-white photographs of diseased leaves (abscissa) and as computed by video image analysis (ordinate) of recorded images of leaves. The line drawn represents the linear regression  $Y = 0.904X + 0.81$ ; coefficient of determination = 0.993 ( $P < 0.01$ ).

of infected foliage. Because measurements of foliar diseases by the automated device are automatically placed in the microcomputer, rapid automatic statistical analysis of results are possible without the further data manipulation required of visual or other assessment methods.

The system described above is a laboratory-based device, but field measurements of exposed symptomatic leaves were accurately analyzed from remotely recorded video images. Unfortunately, symptomatic leaves of many foliar diseases are within the plant canopy where they remain unexposed to remote sensing, and are therefore not included in the sample from which mean disease severity values are estimated. Disease assessment based upon remotely recorded video images may not be accurately applied in this situation.

The entire automated disease assessment device described here is relatively inexpensive (~\$3,000). Since it utilizes an Apple II Plus microcomputer common in many laboratories, it can be implemented very inexpensively in laboratories already possessing this microcomputer.

The possible uses of video image analysis in plant pathology research are many and varied. Since both total and necrotic leaf area of intact plants can be monitored by video image analysis, this procedure is useful for in situ measurements of plant growth as influenced by plant pathogens or of the dynamics of lesion expansion of many foliar pathogens. Quantitative measurements of disease severity by procedures such as digital video image analysis will be helpful in testing and developing models of quantitative epidemiology, in studies of plant pathogens as biological control agents of undesirable host plants, and in studies relating disease severity to crop losses.

#### LITERATURE CITED

- Anonymous. 1947. The measurement of potato blight. *Trans. Br. Mycol. Soc.* 31:140-141.
- Anonymous. 1970. Crop loss assessment methods; FAO manual on the evaluation and prevention of losses by pests, diseases and weeds. Publ. AGP:CP/22. Rome. (Looseleaf).
- Blanchette, R. A. 1982. New technique to measure tree defect using an image analyzer. *Plant Dis.* 66:394-397.
- Brenchley, G. H. 1968. Aerial photography for the study of plant diseases. *Annu. Rev. Phytopathol.* 6:1-22.
- Broderick, H. T., Longshaw, T. B., and Van Lelyveld, L. J. 1973. Disease detection with spectral analysis. Abstr. 073. *Proc. 2nd Int. Cong. Plant Pathol.*
- Chester, K. S. 1950. Plant disease losses: Their appraisal and interpretation. *Plant Dis. Rep. Suppl.* 193:189-362.
- Cobb, N. A. 1892. Contribution to an economic knowledge of the Australian rusts (Uredineae). *Agric. Gaz. N.S. Wales* 3:60-68.
- Croxall, H. E., Gwynne, D. C., and Jenkins, J. E. E. 1952. The rapid assessment of apple scab on leaves and fruit. *Plant Pathol.* 1:39-41.
- Eyal, Z., and Brown, M. B. 1976. A quantitative method for estimating density of *Septoria tritici* pycnidia on wheat leaves. *Phytopathology* 66:11-14.
- Gausman, H. W. 1974. Leaf reflectance of near infrared. *Photogramm. Eng.* 40:182-191.
- Henninger, J., and Hildebrandt, C. 1980. Bibliography of publications on damage assessment in forestry and agriculture by remote sensing techniques. 2nd ed. University of Freiburg, West Germany. 280 pp.
- Horsfall, J. G. 1945. Some problems of data assessment. Pages 38-41 in: *Fungicides and Their Action*. Chronica Botanica Co., Waltham, MA.
- Horsfall, J. G., and Barratt, R. W. 1945. An improved grading system for measuring plant diseases. (Abstr.) *Phytopathology* 35:655.
- Jackson, R. 1964. Detection of plant disease symptoms by infrared photography. *J. Biol. Photogr. Assoc.* 32:45-58.
- Jackson, H. R., Hodgson, W. A., Wallen, V. R., Philpotts, L. E., and Hunter, J. 1971. Potato late blight intensity levels as determined by microdensitometer studies of false-color-aerial photographs. *J. Biol. Photogr. Assoc.* 39:101-106.
- James, W. C. 1971. An illustrated series of assessment keys for plant diseases, their preparations and usage. *Can. Plant Dis. Surv.* 51:39-65.
- James, W. C. 1974. Assessment of plant diseases and losses. *Annu. Rev. Phytopathol.* 12:27-48.
- Large, E. C. 1966. Measuring plant disease. *Annu. Rev. Phytopathol.* 4:9-28.
- Large, E. C., and Doling, D. A. 1962. The measurement of cereal



- mildew and its effect on yield. *Plant Pathol.* 11:47-57.
20. Large, E. C., and Honey, J. K. 1955. Survey of common scab of potatoes in Great Britain, 1952 and 1953. *Plant Pathol.* 4:1-8.
  21. Lindow, S. E., and Webb, R. R. 1981. Use of digital video image analysis in plant disease assessment. (Abstr.) *Phytopathology* 71:891.
  22. Lindow, S. E., and Webb, R. R. 1983. Measurement of foliar plant disease using microcomputer controlled digital video image analysis. *Phytopathology* 73:520-524.
  23. Manzer, F. E., and Cooper, G. R. 1982. Use of portable videotaping for aerial infrared detection of potato diseases. *Plant Dis.* 66:665-667.
  24. Melchers, L. E., and Praker, J. H. 1922. Rust resistance in winter-wheat varieties. U.S. Dep. Agric. Bull. 1046.
  25. Nilsson, H. E. 1980. Application of remote sensing methods and image analysis at macroscopic and microscopic levels in plant pathology. Pages 76-84 in: *Crop Loss Assessment*. Minnesota Agric. Exp. Stn. Misc. Publ. 7.
  26. Odle, W. C., and Toler, R. W. 1976. Remote sensing of St. Augustine-grass decline disease. Remote Sensing Center TR-77, Texas A&M Univ., College Station. 164 pp.
  27. Peterson, R. F., Campbell, A. B., and Hannah, A. E. 1948. A diagrammatic scale for estimating rust intensity on stems and leaves of cereals. *Can. J. Res. C.* 26:496-500.
  28. Sherwood, R. T., Berg, C. C., Hoover, M. R., and Zeiders, K. E. 1983. Illusions in visual assessment of *Stagonospora* leafspot of orchardgrass. *Phytopathology* 73:173-177.
  29. Toler, R. W., Smith, B. D., and Harlan, J. C. 1981. Use of aerial color infrared photography to evaluate crop disease. *Plant Dis.* 65:24-31.
  30. Ullstrup, A. J., Elliott, C., and Hoppe, P. E. 1945. Report of the committee on methods for reporting corn disease ratings. Wash. Div. Cereal Crops Dis., U.S. Dep. Agric., Washington, DC. 5 pp.
  31. Wallen, V. R., and Jackson, H. R. 1971. Aerial photography as a survey technique for the assessment of bacterial blight of field beans. *Can. Plant Dis. Surv.* 51:163-169.
  32. Webb, R. R., and Lindow, S. E. 1981. Evaluation of *Ascochyta pteridium* as a potential biological control agent of bracken fern. (Abstr.) *Phytopathology* 71:911.